

The Histologic Basis of Late Gadolinium Enhancement Cardiovascular Magnetic Resonance in Hypertrophic Cardiomyopathy

James C. C. Moon, MB, BCH,* Emma Reed,† Mary N. Sheppard, FRCPATH,†
Andrew G. Elkington, MB, BCH,* Siew Yen Ho, PhD, FRCPATH,‡ Margaret Burke, MB, FRCPATH,†
Mario Petrou, PhD, FRCS,§ Dudley J. Pennell, MD, FRCP, FESC, FACC*

London, United Kingdom

OBJECTIVES	We sought to identify the histologic basis of myocardial late gadolinium enhancement cardiovascular magnetic resonance (CMR) in hypertrophic cardiomyopathy (HCM).
BACKGROUND	The histologic basis of late gadolinium CMR in patients with HCM is unknown.
METHODS	A 28-year-old male patient with HCM and heart failure underwent late gadolinium enhancement CMR and, 49 days later, heart transplantation. The explanted heart was examined histologically for the extent of collagen and disarray, and the results were compared with a previous in vivo CMR scan.
RESULTS	Overall, 19% of the myocardium was collagen, but the amount per segment varied widely ($SD \pm 19$, range 0% to 71%). Both disarray and collagen were more likely to be found in the mesocardium than in the endo- or epicardium. There was a significant relationship between the extent of late gadolinium enhancement and collagen ($r = 0.7$, $p < 0.0001$) but not myocardial disarray ($p = 0.58$). Segments containing $>15\%$ collagen were more likely to have late gadolinium enhancement. Regional wall motion was inversely related to the extent of myocardial collagen and late gadolinium enhancement but not disarray ($p = 0.0003$, 0.04 , and NS, respectively).
CONCLUSIONS	In this patient with HCM and heart failure, regions of myocardial late gadolinium enhancement by CMR represented regions of increased myocardial collagen but not disarray. (J Am Coll Cardiol 2004;43:2260-4) © 2004 by the American College of Cardiology Foundation

Late gadolinium enhancement cardiovascular magnetic resonance (CMR) can detect regions of myocardial infarction (1,2). Regions of myocardial late gadolinium enhancement also occur in hypertrophic cardiomyopathy (HCM) (3), and the extent of enhancement has been associated with clinical markers of sudden death risk and progression to heart failure (4). The gadolinium contrast agents currently used for late enhancement imaging distribute in the extracellular space, and such regions of enhancement in HCM may represent increased myocardial collagen or the disarray known to occur in this condition (5-8). To date, there has been no histologic correlation of late gadolinium enhancement in HCM. We present the first such correlation from the explanted heart of a patient with HCM who underwent heart transplantation shortly after CMR.

Patient. A 28-year-old man presented with new-onset heart failure. He had been previously fit and healthy. Echocardiography demonstrated left ventricular (LV) hypertrophy, dilation, and poor LV function. Cine CMR demonstrated dilation with severe impairment of systolic function (ejection fraction 12% [normal $>56\%$], end-

diastolic volume 536 ml [normal 77 to 195], end-systolic volume 472 ml [normal 19 to 72]). The maximum wall thickness was 17 mm, and there was severe LV hypertrophy, with a mass index of 272 g/m^2 (normal <113). Late gadolinium CMR demonstrated extensive regions of myocardial enhancement amounting to 30% of the LV myocardium. The patient's condition deteriorated, requiring the insertion of a LV assist device and subsequent heart transplantation 49 days after the CMR scan. The explanted heart showed severe LV hypertrophy and macroscopic scarring. The epicardial coronary arteries were normal. Microscopy showed multiple areas of myocyte/myofibril disarray, mainly in the mesocardial layer, and numerous scars. There was also an increase in fine interstitial fibrosis in areas without disarray, as well as plexiform fibrosis in some of the areas with disarray. Perivascular fibrosis was also present. The findings were diagnostic of HCM in a dilated phase.

CMR. This was performed as previously described (4). Briefly, imaging was performed on a 1.5-T scanner (Siemens Sonata, Erlangen, Germany). Fast imaging at steady-state precession (FISP) cines were acquired in the two- and four-chamber views and multiple contiguous short-axis planes (7-mm slice thickness, 3-mm gap) from the atrio-ventricular ring plane to the apex. A peripheral bolus injection of gadolinium-diethylenetriamine pentaacetic acid (DTPA) (0.1 mmol/kg) was then given, and late gadolinium images were acquired after 10 min, using a segmented

From the *Centre for Advanced Magnetic Resonance in Cardiology (CAMRIC), †Department of Histopathology, ‡Department of Paediatrics, and §Department of Cardiothoracic Surgery, Royal Brompton and Harefield Hospitals, London, United Kingdom. The CAMRIC (Cardiovascular Initiative Grant) and Dr. Moon (Junior Research Fellowship) were supported by the British Heart Foundation.

Manuscript received June 18, 2003; revised manuscript received February 18, 2004, accepted March 2, 2004.

Abbreviations and Acronyms

CMR = cardiovascular magnetic resonance
HCM = hypertrophic cardiomyopathy
LV = left ventricle/ventricular
RV = right ventricular

inversion-recovery sequence (9). Pixel size was 1.7×1.4 mm.

Specimen preparation. Routine fixation was performed with 10% formol saline. Using morphologic landmarks, three short-axis myocardial slices (base, mid, and apical) correlating with specific CMR slices were selected. After photography, each slice was divided into eight contiguous LV tissue blocks and prepared for routine processing to paraffin wax. Two tissue sections ($5 \mu\text{m}$) were cut per block. One was stained with sirius red (picrosirius red), which stains collagen red and myocytes yellow (10,11), and the other with Masson's trichrome stain, which stains collagen blue and myocytes red. The sirius red sections were used for collagen quantification, and the Masson's trichrome sections

for disarray quantification. After collagen quantification, the sirius red slides were digitally scanned and reorganized to recreate the three ventricular short-axis slices.

Data analysis. Analysis was performed independently for the histologic and CMR studies, with researchers for histology blinded to the CMR results, and vice versa. Each of the 24 sirius red-stained blocks were divided into subendocardial, mesocardial, and subepicardial layers, making 72 segments. The trabeculated myocardium was not included. The area of sirius red staining in each segment was quantified using manual planimetry with area quantification and expressed as a percentage of total myocardium in that segment. The percentage of myocytes demonstrating disarray was quantified. The presence of gross macroscopic scarring was determined by the agreement of two observers.

For CMR, the regional wall motion was assessed by the agreement of two observers on a 4-point scale (0 = normal; 1 = mild/moderate hypokinesia; 2 = severe hypokinesia; 3 = akinesia). There were no dyskinetic segments. Late gadolinium enhancement was analyzed in two ways. Objective pixel quantification was performed with assessment of

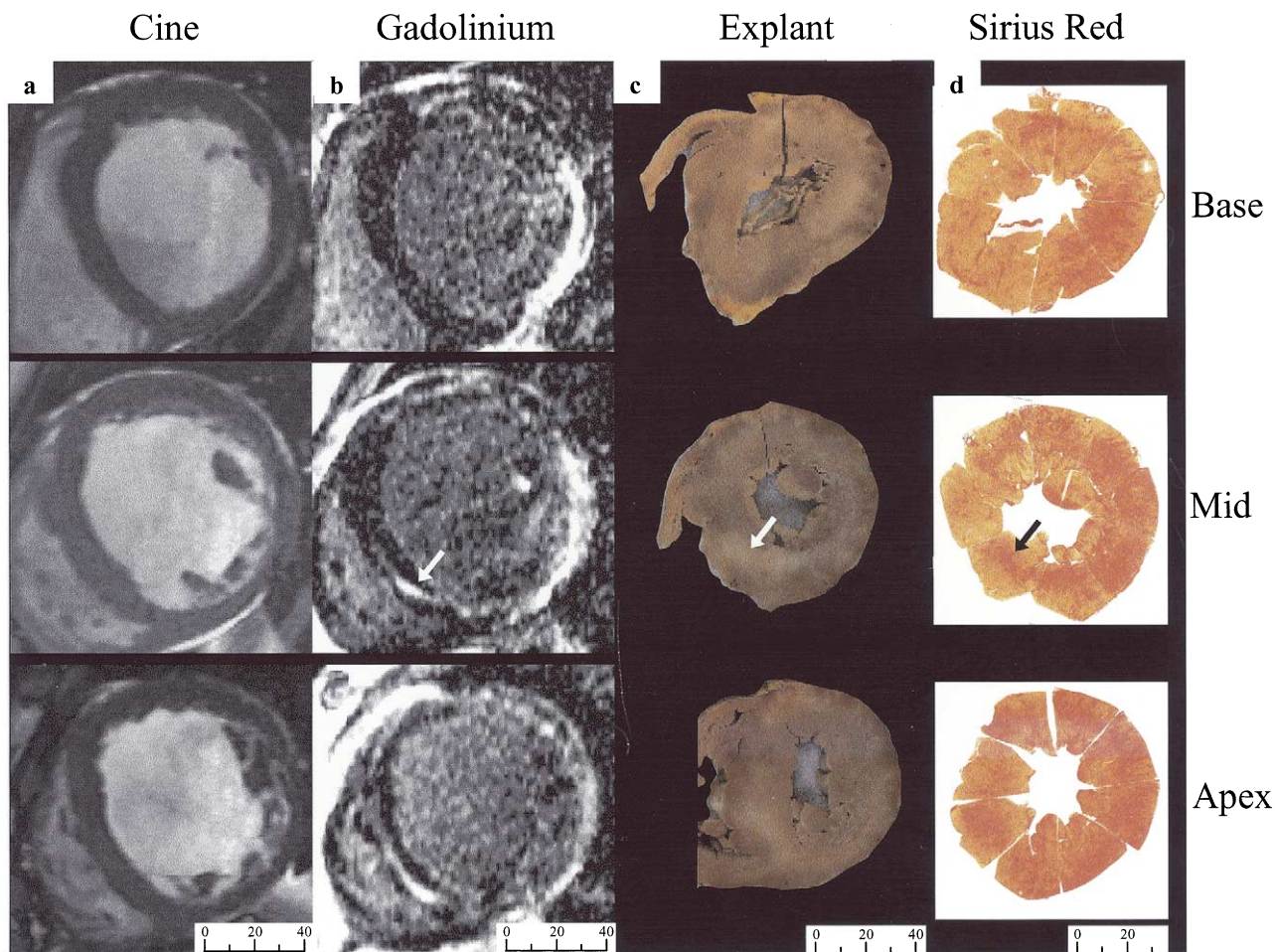


Figure 1. Comparison of (a) in vivo diastolic cine image, (b) in vivo gadolinium-enhanced cardiovascular magnetic resonance, (c) gross specimen of sections from an explanted heart, and (d) histologic sections stained with sirius red. All images are to the same scale. After fixation, considerable contraction has occurred. Regions of gadolinium enhancement correlate with regions of macroscopic unstained pale myocardium and regions of red-stained collagen. A representative mesocardial region, which is well defined, is marked by an arrow.

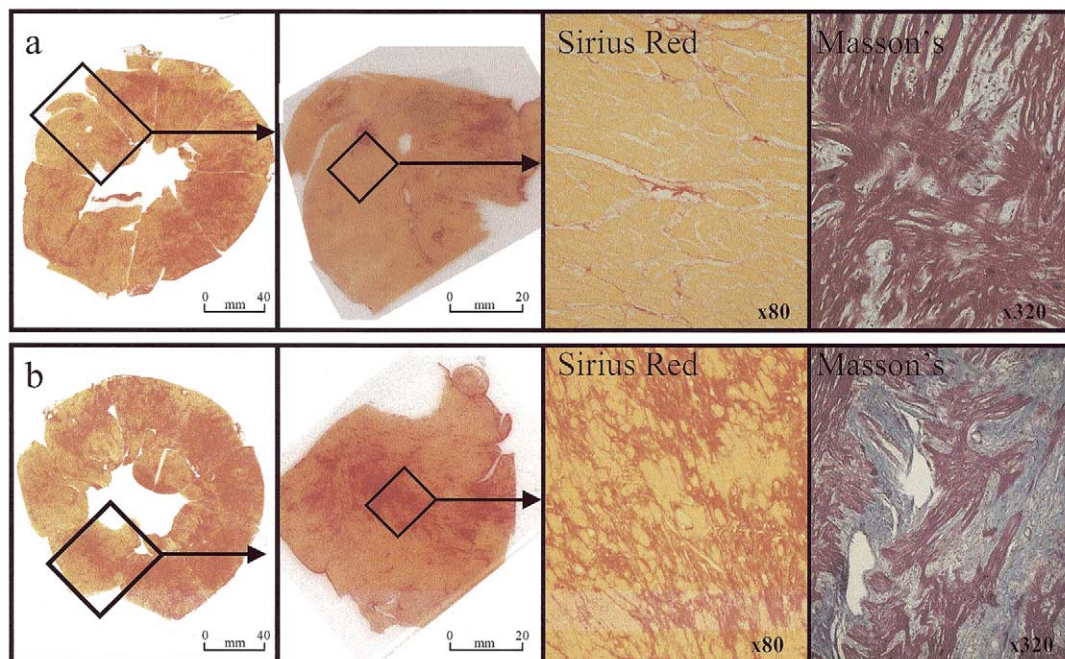


Figure 2. The range of histologic findings. Reading from **left to right**: **column 1** shows the macroscopic appearance of the basal two short-axis slices stained with sirius red, as shown in **Figure 1**. **Column 2** shows a magnification of the **box in column 1**. **Columns 3 and 4** show a magnification of the **box in column 2** stained with sirius red and Masson's trichrome, respectively. **Row a** shows an area that had no late gadolinium enhancement, and there was only 3% collagen but extensive disarray (50%). **Row b** shows an area that had late gadolinium enhancement (arrows in **Fig. 1**), and the mesocardium had macroscopically scarring and extensive collagen (32%) and extensive disarray (50%).

the segmental percentage of enhanced pixels (defined as myocardium with an image intensity of >2 SD above the mean value for remote myocardium). As this technique does not reflect standard clinical assessment of enhancement, visual assessment was also performed by two observers using a three-point scale (enhancement absent, intermediate, or present). The results of the two observers were combined to give a five-point scale.

Linear regression was used to compare the extent of collagen, disarray, and enhancement. Nonparametric Wilcoxon rank comparisons were used for paired group comparisons. For comparison of function with enhancement, collagen, or disarray, a mean transmural score was taken by averaging the epi-, meso-, and endocardial scores before testing. A nonparametric version of the analysis of variance test (Kruskal-Wallis) was used to compare the percentage of collagen in different groups of visual gadolinium enhancement.

RESULTS

The comparative sections by cine and late gadolinium CMR are shown next to the ex vivo macroscopic sections and reconstructed, stained histologic samples in **Figure 1**. The explanted heart has contracted down relative to the in vivo CMR due to the effects of formalin fixation. Examination of morphologic features such as right ventricular (RV) insertion, RV and LV trabeculations, and papillary muscles demonstrate the parity of the in vivo and ex vivo slice

positions. Regions of gross scarring can be seen in the macroscopic explanted slices before staining, although there is also some fixation artifact. A comparison of the late gadolinium images, macroscopic slices, and histologic samples showed concordance between the regions of enhancement and collagen.

Histology. Overall, 19% of the myocardium was collagen. The extent of collagen varied widely between segments ($SD \pm 19$, range 0% to 71%). There was more collagen in the mesocardium than in the endocardium (26% vs. 14%, $p = 0.01$) or epicardium (26% vs. 16%, $p = 0.04$). The extent of disarray varied widely between segments: 3 (4%) segments showed no disarray and 23 (32%) segments had extensive disarray. There was more disarray in the mesocardium than in the endocardium ($p = 0.02$) or epicardium ($p < 0.001$). Myocardial disarray was found to be independent of collagen ($r = 0.1$, $p = 0.45$) (**Fig. 2**).

Macroscopic scars. Ten segments demonstrated macroscopic scarring. These segments had more collagen (41% vs. 15%, $p = 0.003$), more disarray (37% vs. 24%, $p = 0.05$), a higher percentage of enhanced pixels (51% vs. 30%, $p = 0.03$), and a higher likelihood of the segment being scored as visually enhanced (0.83 vs. 0.48, $p = 0.006$).

Collagen, disarray, and enhancement. As the degree of segmental collagen increased, there was a linear increase in the percentage of enhanced pixels ($r = 0.7$, $p < 0.0001$) (**Fig. 3**), as well as the likelihood of the segment being scored as visually enhanced ($p = 0.0001$) (**Fig. 3B**). There

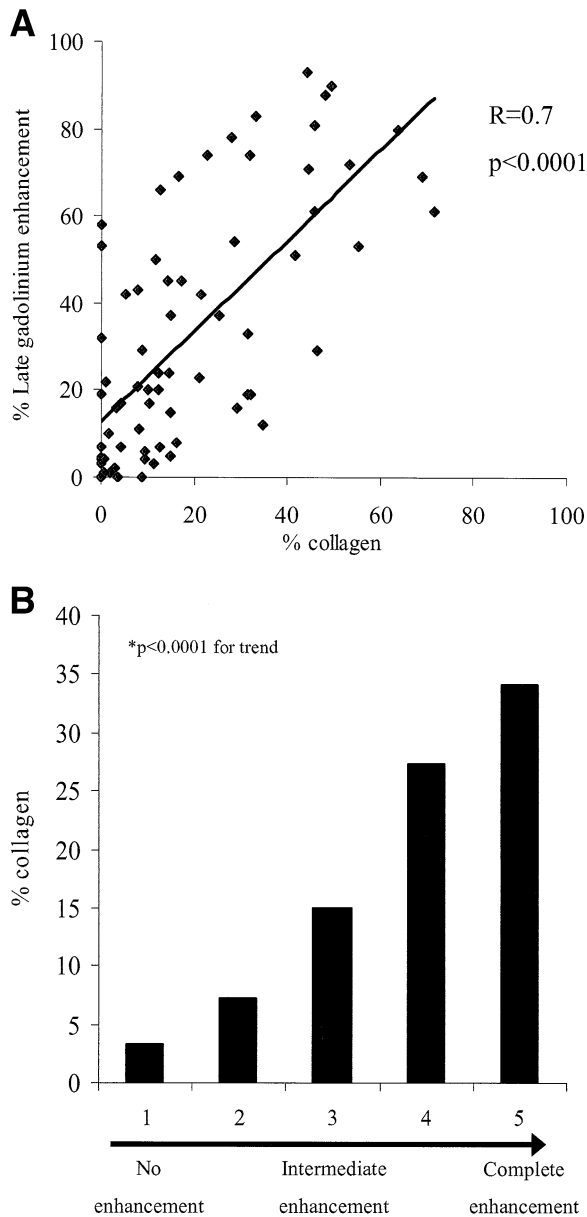


Figure 3. (A) The quantitative relationship between the percentage of pixels per segment showing late gadolinium enhancement and the percentage of collagen. (B) The qualitative relationship between the segmental scoring of late gadolinium enhancement and the percentage of collagen.

was no relationship between disarray and the percentage of enhanced pixels ($p = 0.58$) or visual enhancement. Segments where both observers agreed there was complete enhancement had a mean collagen score of 34%, whereas when both observers agreed that there was no segmental enhancement, the mean collagen score was 3%. At a mean percentage collagen of 15%, segments were more likely to be scored as visually enhanced (Fig. 3B).

Function. Regional wall motion was inversely related to the extent of myocardial collagen and gadolinium enhancement but not disarray ($p = 0.0003, 0.04,$ and NS, respectively).

DISCUSSION

Late gadolinium enhancement CMR relies on the delivery to the myocardium of intravenous gadolinium chelate, which is a biologically inert tracer that freely distributes in extracellular water but is unable to cross the intact cell membrane. Due to a combination of increased volume of distribution in fibrosis and slower washout kinetics, there is a relative accumulation of gadolinium in areas of expanded extracellular space in comparison with normal myocardium, which can be detected in the late washout phase (12,13). The expanded extracellular space in the myocardium can be caused by various components such as fibrosis, protein infiltration, or possibly myocardial disarray with disorganized myocardial fiber packing. This is the first report confirming the relationship between the presence of myocardial late gadolinium enhancement in HCM and myocardial collagen, which is a major component of myocardial fibrosis.

Although HCM is caused by mutation in genes encoding components of the sarcomere, an important component of phenotypic expression is thought to be due to increased myocardial connective tissue, a principal component of which is collagen (14,15). Different patterns of fibrosis have been observed (16). There may be a generalized increase in the normal structural skeletal framework of the myocardium (pericellular, intercellular, and fascicular connective tissue). In extreme cases, individual myocytes may become encased in collagen. In addition, there may be fibrosis associated with myocardial disarray (plexiform fibrosis), particularly at the RV insertion points (17), perivascular fibrosis, and microscopic replacement scars. However, our knowledge of the histology of HCM is derived principally from ex vivo study of patients who have died of their disease. Late gadolinium-enhanced CMR may be considered a form of in vivo histologic assessment, with the additional advantages that it can be performed in patients with any HCM phenotype with global myocardial coverage and serially to potentially monitor disease progression.

Myocardial enhancement in HCM has been demonstrated in both minimally symptomatic individuals and individuals at high risk of sudden death or myocardial thinning and dilation (3,4). In a study of minimally symptomatic individuals, the mean extent of enhancement was 8% (3). In a recent study of 53 individuals with HCM, patients with progressive LV dilation had more enhancement than controls (28.5% vs. 8.7%, $p < 0.001$), as did patients with two or more risk factors for sudden death (15.7% vs. 8.6%) (4). Furthermore, different distributions of enhancement have been reported with minimally symptomatic individuals, with enhancement limited to the RV insertion points. Our patient had 30% myocardial enhancement, with multifocal areas of confluence, both of which have been linked to progressive disease. Strictly, the correlations found here should not be applied to RV insertion point enhancement, as this may represent focal plexiform

fibrosis with disarray. Further correlations are awaited, but this may take time because of the relatively low annual mortality or need for transplantation in HCM patients. Interestingly, our data show that in HCM, regions of enhancement may not represent complete replacement by fibrosis, but rather areas of focally increased collagen content.

Study limitations. This patient had an extreme phenotype of HCM. This was inevitable because the study could only have been performed if the patient had either died or undergone heart transplantation. The *ex vivo* contraction of the ventricle made alignment of *in vivo* imaging and histology imperfect and may have resulted in an underestimate of the strength of the relationship between collagen and enhancement. Myocardial enhancement can be found in other cardiomyopathies (18,19), and this may also represent fibrosis, but this is unproven, especially in the infiltrative diseases. Future work is needed to determine the prognostic and diagnostic implications of myocardial enhancement in these conditions.

Acknowledgments

The authors thank Professors P. Poole-Wilson and W. McKenna for their help and support during the preparation of this manuscript.

Reprint requests and correspondence: Dr. Dudley J. Pennell, Professor of Cardiology, CMR Unit, Royal Brompton Hospital, Sydney Street, London SW3 6NP, United Kingdom. E-mail: d.pennell@ic.ac.uk.

REFERENCES

1. Kim RJ, Wu E, Rafael A, et al. The use of contrast-enhanced magnetic resonance imaging to identify reversible myocardial dysfunction. *N Engl J Med* 2000;343:1445-53.
2. Wu E, Judd RM, Vargas JD, Klocke FJ, Bonow RO, Kim RJ. Visualisation of presence, location, and transmural extent of healed Q-wave and non-Q-wave myocardial infarction. *Lancet* 2001;357:21-8.
3. Choudhury L, Mahrholdt H, Wagner A, et al. Myocardial scarring in asymptomatic or mildly symptomatic patients with hypertrophic cardiomyopathy. *J Am Coll Cardiol* 2002;40:2156-64.
4. Moon JCC, McKenna W, McCrohon JA, Elliott PM, Smith GC, Pennell DJ. Toward clinical risk assessment in hypertrophic cardiomyopathy with gadolinium cardiovascular magnetic resonance. *J Am Coll Cardiol* 2003;41:1561-7.
5. Kim RJ, Judd RM. Gadolinium-enhanced magnetic resonance imaging in hypertrophic cardiomyopathy: *in vivo* imaging of the pathologic substrate for premature cardiac death? *J Am Coll Cardiol* 2003;41:1568-72.
6. Maron BJ. Hypertrophic cardiomyopathy: a systematic review. *JAMA* 2002;287:1308-20.
7. Basso C, Thiene G, Corrado D, Buja G, Melacini P, Nava A. Hypertrophic cardiomyopathy and sudden death in the young: pathologic evidence of myocardial ischemia. *Hum Pathol* 2000;31:988-98.
8. Emoto R, Yokota Y, Miki T, et al. Prognosis of hypertrophic cardiomyopathy: echocardiographic and postmortem histopathologic study of 30 patients. *J Cardiol* 1988;18:695-703.
9. Simonetti OP, Kim RJ, Fieno DS, et al. An improved MR imaging technique for the visualization of myocardial infarction. *Radiology* 2001;218:215-23.
10. Puchtler H, Waldrop FS, Valentine LS. Polarization microscopic studies of connective tissue stained with picro-sirius red. *Beitr Pathol* 1973;150:174-87.
11. Junqueira LC, Bignolas G, Brentani RR. Picrosirius staining plus polarization microscopy, a specific method for collagen detection in tissue sections. *Histochem J* 1979;11:447-55.
12. Kim RJ, Chen EL, Lima JAC, Judd RM. Myocardial Gd-DTPA kinetics determine MRI contrast enhancement and reflect the extent and severity of myocardial injury after acute reperfused infarction. *Circulation* 1996;94:3318-26.
13. Flacke SJ, Fischer SE, Lorenz CH. Measurement of the gadopentetate dimeglumine partition coefficient in human myocardium *in vivo*: normal distribution and elevation in acute and chronic infarction. *Radiology* 2001;218:703-10.
14. Shirani J, Pick R, Roberts WC, Maron BJ. Morphology and significance of the left ventricular collagen network in young patients with hypertrophic cardiomyopathy and sudden cardiac death. *J Am Coll Cardiol* 2000;35:36-44.
15. Kitamura M, Shimizu M, Ino H, et al. Collagen remodeling and cardiac dysfunction in patients with hypertrophic cardiomyopathy: the significance of type III and VI collagens. *Clin Cardiol* 2000;24:325-9.
16. Anderson KR, Sutton MG, Lie JT. Histopathological types of cardiac fibrosis in myocardial disease. *J Pathol* 1979;128:79-85.
17. Kuribayashi T, Roberts WC. Myocardial disarray at junction of ventricular septum and left and right ventricular free walls in hypertrophic cardiomyopathy. *Am J Cardiol* 1992;70:1333-40.
18. McCrohon JA, Moon JCC, Prasad SK, et al. Differentiation of heart failure related to dilated cardiomyopathy and coronary artery disease using gadolinium enhanced cardiovascular magnetic resonance. *Circulation* 2003;108:54-9.
19. Moon JC, Mundy HR, Lee PJ, Mohiaddin RH, Pennell DJ. Images in cardiovascular medicine: myocardial fibrosis in glycogen storage disease type III. *Circulation* 2003;107:E47.